

CHAPTER - V

DISSOLUTION OF CALCITE IN ORGANIC ACIDS - II
(effect of temperature)

CHAPTER - V

DISSOLUTION OF CALCITE IN ORGANIC ACIDS - II

(Effect of temperature)

	<u>Page</u>
5.1 Introduction 	99
5.2 Experimental 	99
5.3 Observations and Results 	100
5.3.1 Effect of temperature on morphology of etch pits ...	100
5.3.2 Effect of temperature on etch rates 	102
5.4 Discussion 	104
5.4.1 Morphology of etch pits ...	104
5.4.2 Mechanism of dissolution ...	107
5.4.3 Nature of Adsorption ...	110
5.4.5 Concentration dependence of pre-exponential factors ...	112
5.4.5 Temperature dependence of peak concentration 	115
5.5 Conclusions 	116

5.1 INTRODUCTION

It is well known that the thermally activated process has a definite value of activation energy. It is also observed that the shape of an etch pit on calcite cleavages is dependent on temperature of etching (Shah, 1976). Further, for a given concentration of an acid, it depends on the activation energy. However, for a given shape of an etch pit produced by etchants of different concentrations the activation energy is not constant (Shah, 1976). The literature available on etching of crystals is almost qualitative in nature. The qualitative nature of work on dissolution phenomena now shows the signs of slackening as it has failed to explain the exact mechanism of dissolution and does not give any idea about the nucleation and shapes of etch pits. In this chapter an attempt is made to understand the mechanism of dissolution and to correlate the results, if possible, with surface micro-morphology of calcite cleavages.

5.2 EXPERIMENTAL

The etching was carried out as mentioned earlier in Chapter 4. The measurements of lengths of etch pits on a crystal surface kept on microscope stage and observed through vertical microscope (Carl Zeiss) were carried out by using a filar micrometer eyepiece ($L.C = 0.2\mu$). An

accuracy of $\pm 0.1 \mu$ can be achieved by this method.

The surface dissolution rate was measured by usual weight-loss method.

5.3 OBSERVATIONS AND RESULTS :

5.3.1 Effect of temperature on morphology of etch pits :

(a) Lactic acid :

Fig. 5.1a and 5.1b show the photomicrographs of calcite cleavage counterparts etched in 0.1479 N (1% by vol.) lactic acid at 35°C for 45 seconds and 60°C for 20 seconds respectively. The shape of an etch pits is rhombic at 35°C whereas it changes to hexagonal at 60°C. The transition takes place approximately at 40°C. However, the transition temperature is not sharply defined. Figs. 5.2a and 5.2b exhibit photomicrographs of oppositely matched cleavage faces etched in 1.479 N (10% by vol.) at 35°C for 15 seconds and at 80°C for 5 seconds respectively. The oval (leaf-like) shape of an etch pit changes to boat shape (fig. 5.2b).

Figs. 5.3a and 5.3b show the photomicrographs of cleavage counterparts etched in 14.79 N (100% by vol.) at 35°C for 12 minutes and at 55°C for 3.3 minutes. There is perfect one-to-one correspondence regarding position of etch pits. Figs. 5.4a and 5.4b show the photomicrographs of cleavage counterparts etched in 14.79N (100% by vol.)

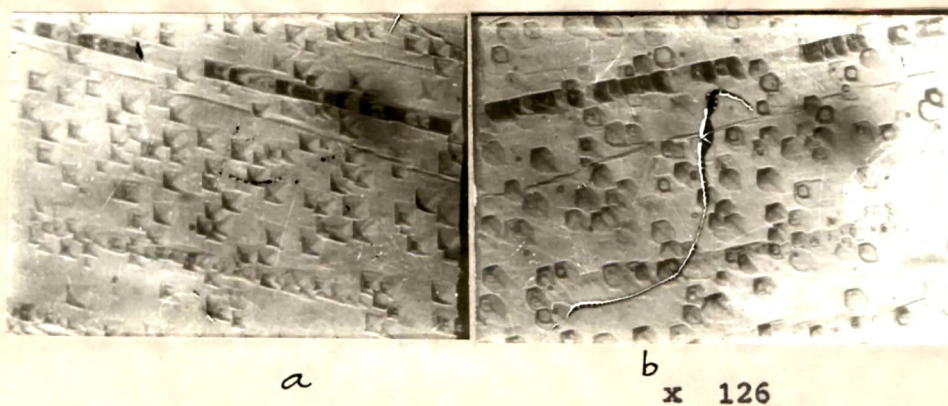
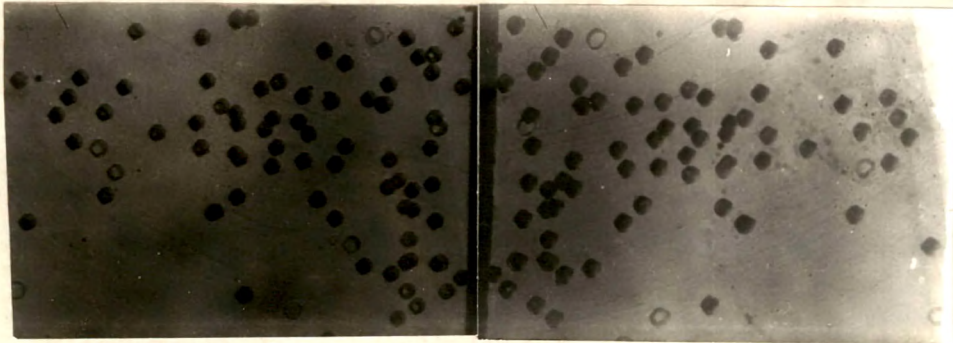


Fig. 5.1 a and b show the photomicrographs of calcite counterparts etched in 0.1479N (1% by vol.) lactic acid at 35°C for 45 seconds and at 60°C for 20 seconds respectively.



x 200

Fig. 5.2 a and b exhibit photomicrographs of oppositely matched cleavage faces etched in 1.479N (10% by Vol.) lactic acid at 35°C for 15 seconds and at 80°C for 5 seconds respectively.



a

b

x 126

Fig. 5.3 a and b show photomicrographs of cleavage counterparts etched in 14.79N (100% by vol.) lactic acid at 35°C for 12 minutes and at 55°C for 3.3 minutes respectively.

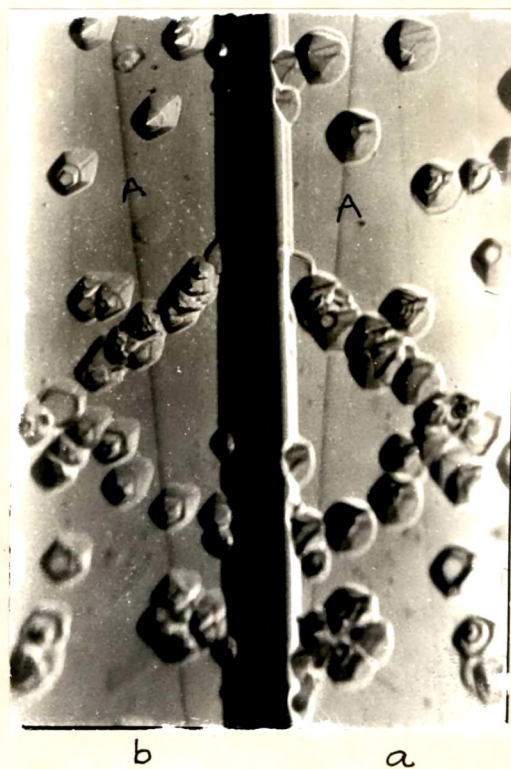


a

b

x 400

Fig. 5.4 a and b show the photomicrographs of cleavage counterparts etched in 14.79N (100% by vol.) lactic acid at 35°C for 12 minutes and at 60°C for 3.3 minutes respectively.



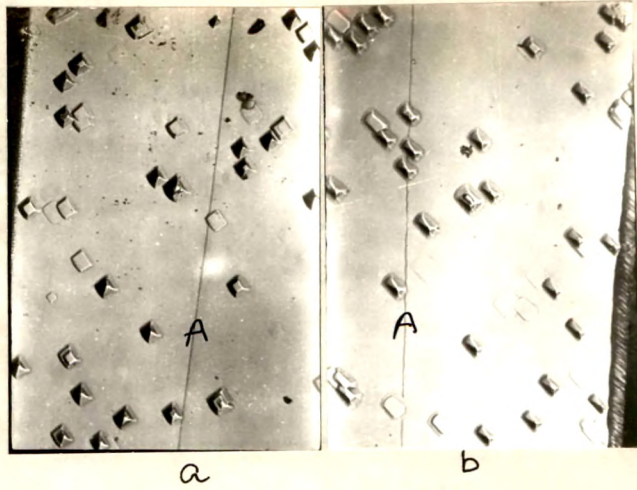
x 300

Fig. 5.5 a and b exhibit photomicrographs of cleavage counterparts etched in 14.79N (100% by vol.) lactic acid at 35°C for 12 minutes at 70°C for 1.7 minutes respectively.

at 35°C for 12 minutes and at 60°C for 3.3 minutes. As the temperature increases, the tip of the pentagonal etch pit becomes prominent (fig. 5.4b) resulting in elongated pentagonal etch pit. Fig. 5.5a and 5.5b exhibit the photomicrographs of cleavage counterparts etched in 14.79^N (100% by vol.) at 35°C for 12 minutes and 70°C for 1.7 minutes. At 70°C, the tip of pentagonal etch pit comes out completely. The cleavage line A (figs. 5.5a and b) shifts slightly on etching. However, there is perfect matching of etch pits. Comparison of figures 5.1, 5.2, 5.3, 5.4 and 5.5 shows that there is improvement in the quality of etch pits with the increase in the concentration of lactic acid. Higher the concentration, better is the quality of etch pits. Similar conclusion was drawn earlier (c.f. Chapter 4).

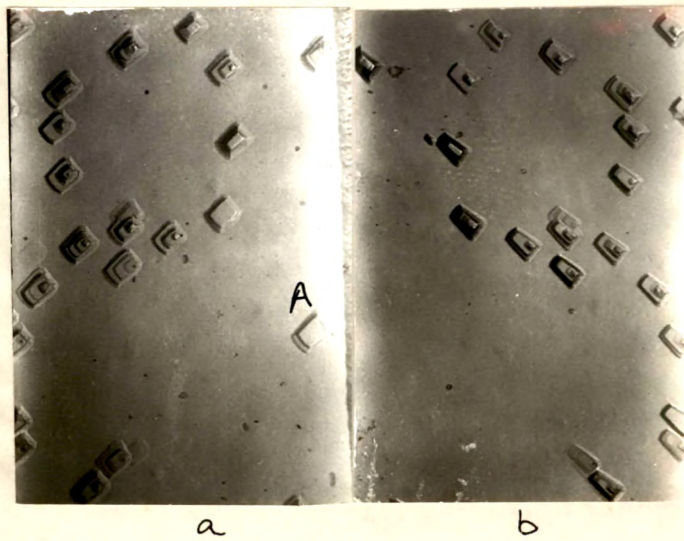
(b) Formic acid :

Figs. 5.6a and 5.6b show the photomicrographs of cleavage counterparts etched in 25.99^N (100% by vol.) formic acid at 35°C for 150 seconds and at 50°C for 60 seconds. There is perfect matching of etch pits on cleavage counterparts with a shift of cleavage lines. The rectangular shape of an etch pit just elongates along [110]. Figs. 5.7a and 5.7b exhibit photomicrographs of matched cleavage surfaces etched in 25.99^N (100% by vol.) at 60°C



x 200

Fig. 5.6 a and b show photomicrographs of cleavage counterparts etched in 25.99N (100% by vol.) formic acid at 35°C for 150 seconds and at 50°C for 60 seconds respectively



x 200

Fig. 5.7 a and b exhibit photomicrographs of cleavage counterparts etched in 25.99N (100% by vol.) formic acid at 60°C for 60 seconds and at 80°C for 15 seconds respectively.

for 60 seconds and at 80°C for 15 seconds respectively. There is perfect matching regarding position of etch pits except pit A (fig. 5.7a). This might be due to unequal stresses applied at an edge while cleaving the crystal. It should be mentioned here that the photograph was taken at the edge of the sample. The shape of an etch pit is basically same at 80°C except that there is some tendency to become elongated pentagon which may be due to very high rate of reaction at 80°C . The shape of an etch pit at lower concentrations of formic acid is an elongated pentagon (cf Chapter 4, figs. 4.10 and 4.11). The etch pit shape is independent of temperature in case of formic acid for the range of temperatures 10°C to 80°C . It should be mentioned here that for lower concentrations an elongated pentagonal shape of an etch pit is also independent of temperature of etching.

5.3.2 Effect of temperature on etch rates :

(a) Lactic acid :

Table 4.3 (cf, Chapter 4) shows the rates of tangential and surface dissolution at various temperatures ranging from 20°C to 80°C for various concentrations of lactic acid. Figs. 5.8 and 5.9 show the graphs of log of etch pit widening rate (V_t) along $[110]$ and surface dissolution rate (V_s) against the reciprocal of temperatures

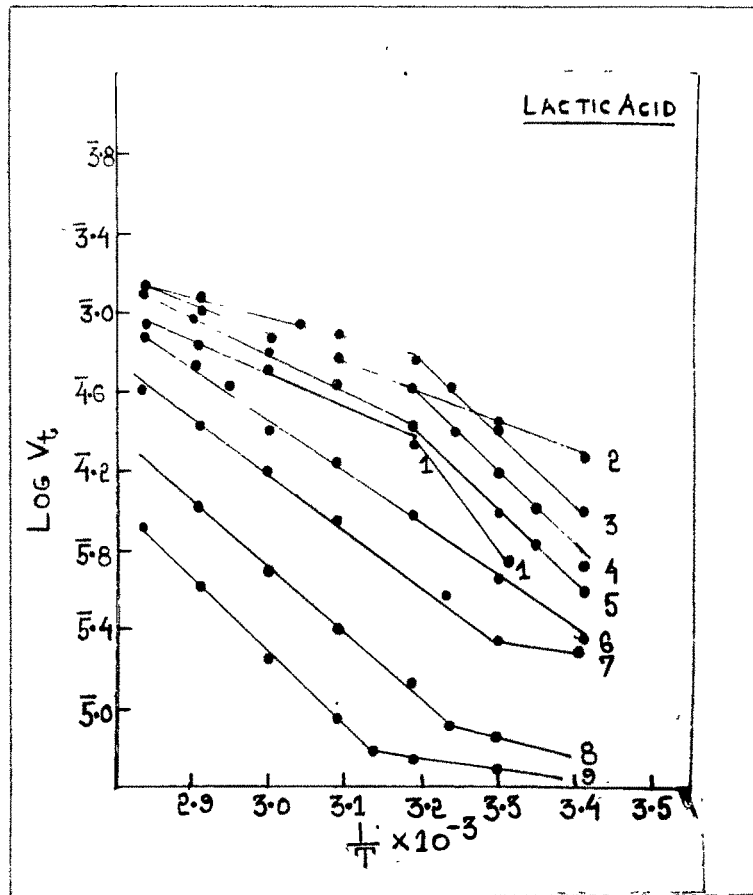


Fig. 5.8 plot of $\log V_t$ versus $1/T$ for various concentrations of lactic acid

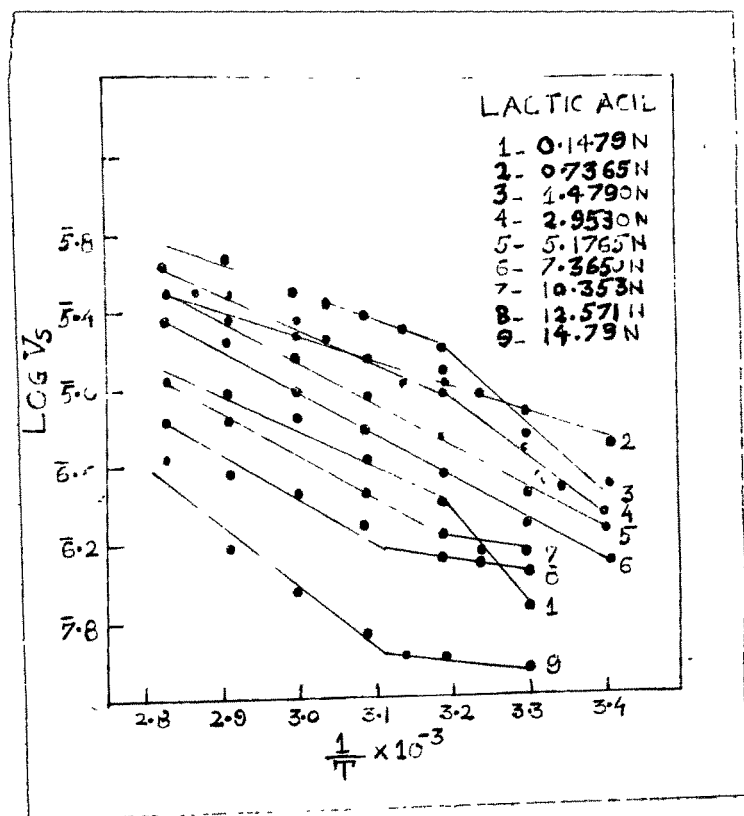


Fig. 5.9 Plot of $\log V_s$ versus $1/T$ for various concentrations of lactic acid.

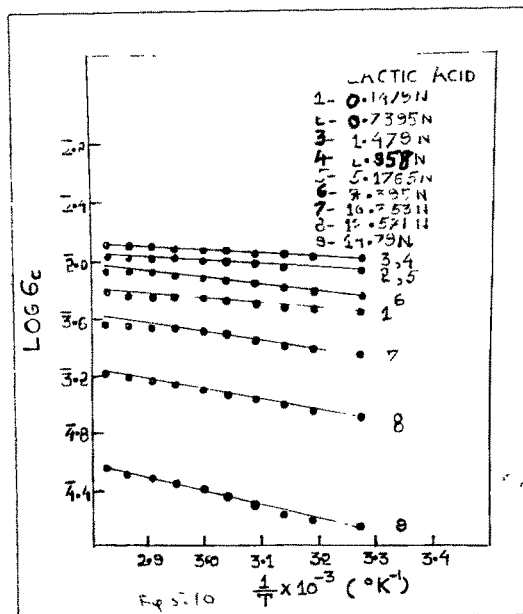


Fig. 5.10 Plot of $\log D_c$ versus $1/T$ for various concentrations of lactic acid.

for various concentrations of lactic acid. According to Arrhenius equation

$$V = A \exp (- E / KT)$$

the slope of the graph of $\log V_t$ (or $\log V_s$) versus $1/T$ represents the value of E/K where E is the activation energy of the reacting species and K is the Boltzmann constant. The straight line graphs split into two regions showing a kink at about 40°C . Hence, the activation energy for each linear portion of the graph is calculated. The energies thus calculated for different linear portions of the graphs for all concentrations of lactic acid are shown in table 5.1 which also shows the log of corresponding pre-exponential factors (A_t and A_s).

Similar Arrhenius type of plots for electrical conductivity (σ_c) are shown in fig. 5.10 (cf table 4.7 Chapter 4). The plots are straight lines. The activation energy for conductivity, E_c , for all concentrations of lactic acid are also listed in table 5.1.

(b) Formic acid :

Table 4.4 (cf, Chapter 4) shows the etch rates V_t and V_s for various concentrations of formic acid in the temperature range of $10 - 60^\circ\text{C}$. Figs. 5.11 and 5.12 show the Arrhenius plots for tangential and surface dissolution rates respectively. The plots are straight lines. The

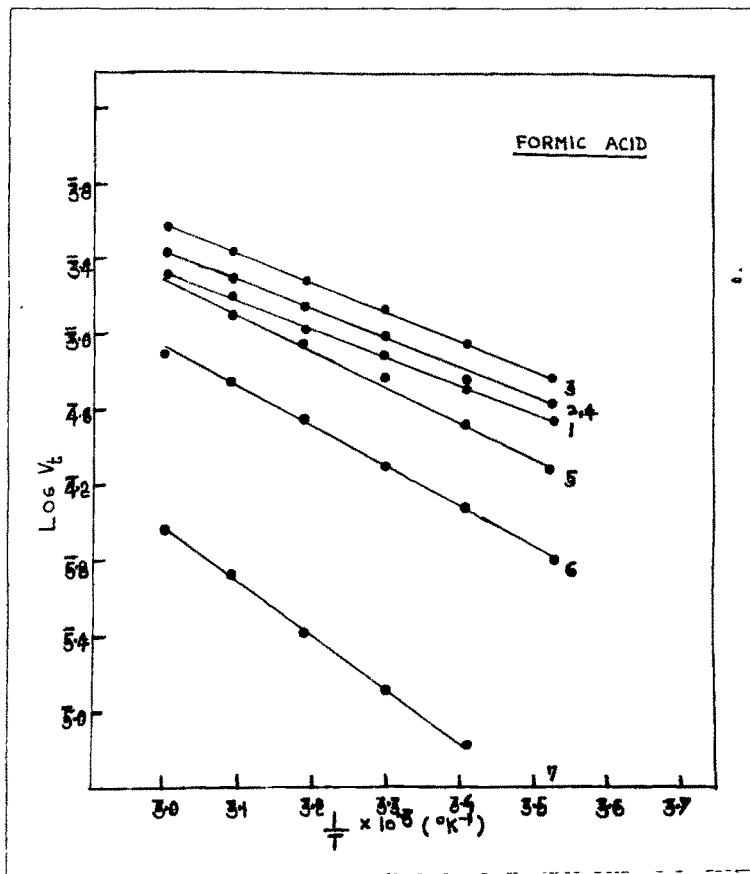


Fig. 5.11 Plot of $\log V_t$ versus $1/T$ for various concentrations of formic acid.

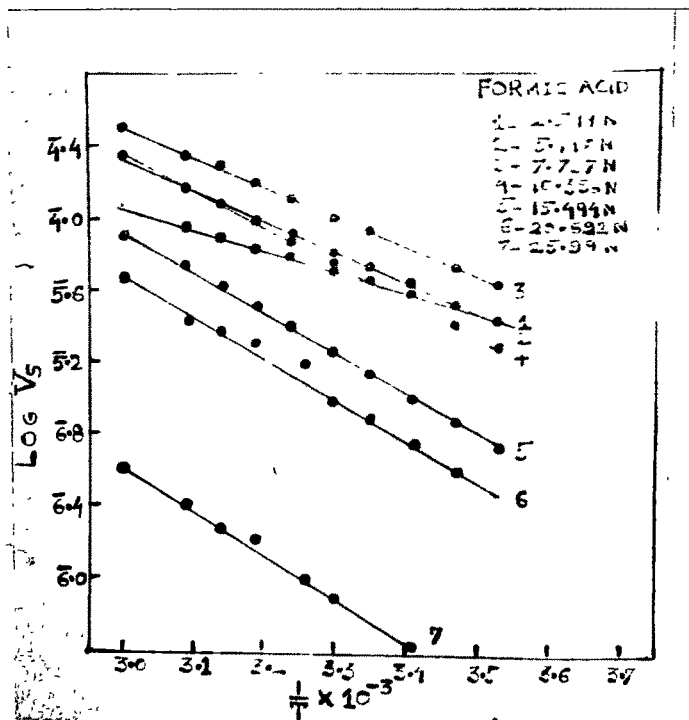


Fig. 5.12 Plot of $\log V_s$ versus $1/T$ for various concentrations of formic acid.

TABLE - 5.1 (Lactic acid)

For temperature of etching less than 40°C									
Conc, % by vol.	Conc, (N)	log C(N)	E_t (ev)	E_s (ev)	E_t/E_s	log A_t	log A_s	E_C (ev)	
1	0.1479	1.1700	0.99	0.95	1.04	-	9.7400	0.04	
5	0.7395	1.8689	0.28	0.27	1.03	1.1000	1.4570	0.04	
10	1.4790	0.1700	0.79	0.59	1.34	9.6000	4.5680	0.04	
20	2.9580	0.4710	0.79	0.59	1.34	9.4000	4.5080	0.04	
35	5.1765	0.7140	0.79	0.44	1.79	9.2000	1.6790	0.04	
50	7.3950	0.8689	0.54	0.44	1.23	3.9000	1.6630	0.08	
70	10.3530	1.0149	0.10	0.09	1.11	4.6600	5.6450	0.09	
85	12.5715	1.0993	0.10	0.09	1.11	4.3800	5.5450	0.10	
100	14.7900	1.1700	0.10	0.09	1.11	4.3000	5.0000	0.18	

TABLE - 5.1 (Cont.)

For temperature of etching greater than 40°C							
Conc., % by Vol.	Conc., N	E_t (ev)	E_s (ev)	$\frac{E_t}{E_s}$	$\log A_t$	$\log A_s$	E_c (ev)
1	0.1479	0.28	0.39	0.72	-	0.7040	0.04
5	0.7395	0.28	0.27	1.03	1.1000	1.6140	0.04
10	1.4790	0.20	0.27	0.74	0.0000	1.5840	0.04
20	2.9580	0.28	0.39	0.72	1.1000	1.1840	0.04
35	5.1765	0.40	0.44	0.91	2.8000	1.6790	0.04
50	7.3950	0.54	0.44	1.23	3.9000	1.6630	0.08
70	10.3530	0.59	0.44	1.34	5.2000	1.3130	0.09
85	12.5715	0.65	0.44	1.48	5.6000	1.1130	0.10
100	14.7900	0.77	0.63	1.22	6.7000	3.4900	0.18

values of activation energies for tangential and surface dissolutions, E_t and E_s , are computed using Arrhenius equation and are listed in table 5.2. Table 5.2 also shows the log of pre-exponential factors A_t and A_s for tangential and surface dissolutions respectively. Fig. 5.13 is the Arrhenius type of plot for electrical conductivity of different concentrations of formic acid (cf, table 4.8, Chapter 4). The values of activation energy for conductivity E_C , are also listed in table 5.2.

5.4 DISCUSSION :

5.4.1 Morphology of etch pits :

Most etchants dissolve a crystal surface independently of line defects producing etch pits. The surface dissolution has been attributed (Gilman 1960, Ives and Plews 1965) to the presence of other short-lived defects such as lattice impurities. It plays important role in the etching process. Hence the determination of the activation energies for dissolution of surface, E_s , and for tangential movement of steps away from the nucleus, E_t , is likely to enhance the understanding of etching process.

The temperature of etching affects the plane shape of etch pits for a definite concentration of the etchant

TABLE - 5.2 (Formic acid)

Conc, % by vol.	Conc, N	log C(N)	E_t (ev)	E_s (ev)	E_t/E_s	log A_t	log A_s	E_c (ev)
10	2.599	0.4148	0.32	0.24	1.33	2.1200	1.6700	0.052
20	5.198	0.7159	0.32	0.30	1.06	2.2800	1.1200	0.040
30	7.797	0.8919	0.32	0.39	0.82	2.4000	2.4100	0.040
40	10.396	1.0165	0.32	0.39	0.82	2.2800	2.2800	0.040
60	15.494	1.1900	0.39	0.43	0.90	2.6600	2.4500	0.040
80	20.692	1.3158	0.42	0.45	0.93	3.2200	2.3900	0.040
100	25.990	1.4148	0.56	0.47	1.19	4.8100	2.2000	0.073

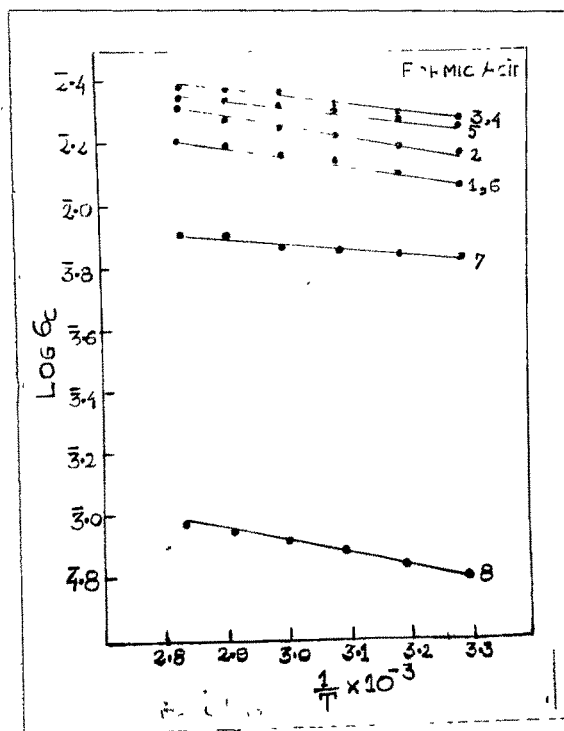


Fig. 5.13 Plot of $\log \sigma_c$ versus $1/T$ for different concentrations of formic acid.

(Shah, 1976). For temperatures within a given temperature range plane shape of an etch pit is invariant within the limits of optical resolution in this range. Hence activation energy is constant. Thus, as the range of temperature changes in a gradual and systematic way, the activation energy also changes. Further, the etch pit shape depends upon the concentration range of the etchant at a constant temperature. This was conclusively established by Mehta (1972) in this laboratory using hydrochloric and glacial acetic acids as the etchants. It is further verified by the present author using lactic and formic acids as the etchants (cf, Chapter 4). Further, the activation energy also depends upon the concentration of the etchant. Table 5.3 shows the various shapes of etch pits produced by various concentrations of lactic and formic acids. It also shows the value of activation energies, E_t . A careful glance at it shows that for a given concentration of lactic acid, the activation energy changes when the shape of an etch pit changes. In case of formic acid, the shape of an etch pit is independent of the temperature of etching. Hence, the activation energy is independent of temperature. However, the same value of activation energy viz. for 1.479N (10% by vol.) below 40°C and for 14.79N (100% by vol.) above 50°C, does not produce same shape of an etch pit. (see fig. 5.2a & 5.5b).

TABLE - 5.3

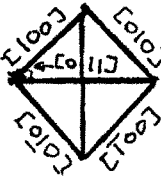
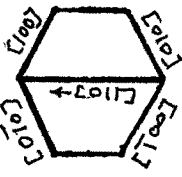
Sr.No.	Shape	Etchant	Conc, Range (N)	Temp. Range (°C)	E_t (ev)
1		Lactic	0 - 0.1479	< 40	0.99
2		Lactic	0 - 0.1479	> 40	0.28
3		Lactic	1.479-5.1765	< 40	0.79
4		Lactic	1.479-5.1765	> 40	0.2 - 0.4

TABLE - 5.3 Cont....

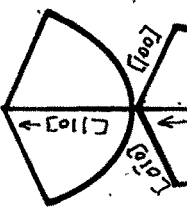
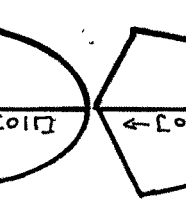
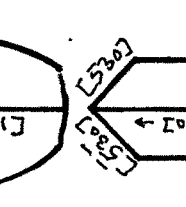
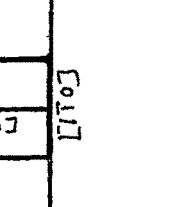
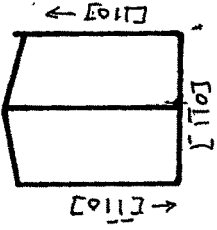
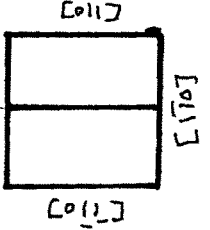
Sr.No.	Shape	Etchant	Conc. Range (N)	Temp. range (°C)	E_t (ev)
5		Lactic	10.353 - 14.79	> 50	0.10
6		Lactic	7.395 - 10.353	> 40	0.54 - 0.59
7		Lactic	14.79	> 55	0.77
8		Formic	< 15.494	10 - 60	0.32

TABLE 5.3 cont..

Sr.No.	Shape	Etchant	Conc. Range (N)	Temp. range (°C)	Et (ev)
9		Formic	15.494	10 - 60	0.39
10		Formic	20.692 - 25.99	10 - 60	0.42 - 0.56

It was established in this laboratory earlier that for the same shape of an etch pit produced by different etchants, the activation energy is not constant (Shah, 1976). For example rhombic shape of etch pit can be produced by 0.45% glacial acetic acid, 1% hydrochloric acid, 1% lactic acid and saturated solution of ammonium chloride. The activation energies, E_t , for rhombic etch pits are 0.68, 0.02, 0.99 and 0.35 electron volts respectively. Similarly, boat-shaped etch pits can be produced by 1.479N (10% by vol.) lactic acid, saturated solutions of potassium and sodium hydroxide pellets (A.J. Shah). The values of activation energies are 0.20, 0.62 and 0.61 electron volts respectively. Therefore, the activation energy is not the only factor which decides the plane shape of an etch pit.

It is also possible to predict about the symmetry and quality of etch pits on calcite cleavage surfaces. It was concluded by Shah (1976) that higher the ratio E_t / E_s better is the quality of etch pits and that the ratio is greater than one. It was stated earlier (cf, Chapter 4) that the quality of an etch pit improves with the concentration of the etchant. A glance at tables 5.1 and 5.2 shows that the ratio E_t / E_s is usually greater

than one. Further for better quality of etch pits the ratio n_t / n_s should also be considered (cf, Chapter 4).

5.4.2 Mechanism of dissolution :

Any catalytic reaction proceeds in the following steps : (Gerasimov et al 1974).

- (i) Diffusion of reacting species,
- (ii) Adsorption on the surface,
- (iii) Reaction on the surface,
- (iv) Desorption of reaction products and
- (v) Diffusion of products away from the surface.

Depending upon the conditions in which the process is conducted in, any reaction can be diffusion controlled or kinetically controlled. The rate of diffusion grows with the temperature according to the law similar to the Arrhenius equation (Gerasimov et al, 1974),

$$D = K \exp (- E / RT) \quad \dots\dots (5.1)$$

It should be noted that the value of E rarely exceeds 1000 - 2000 calories per mole (0.05 - 0.10 ev) i.e. it is only a small fraction of the activation energies of

most of the reactions. Consequently, the rate of diffusion will increase with temperature considerably slower than the rate of chemical reaction. Viscosity and diffusion are correlated (Laidler, 1950). Whether or not the process is diffusion controlled can be decided by plotting $\log \delta$ (where δ is the viscosity of the etchant) versus $1/T$. For liquids which have low viscosity at room temperature, the value of activation energy, E_{δ} , is usually 0.14 ev. For denser solutions the graph of $\log \delta$ vs $1/T$ consists of two straight lines having different slopes, each corresponding to relatively high value of activation energy (Sangwal and Arora, 1978). If E_{δ} and activation energy of dissolution happen to be equal, the dissolution kinetics are fully diffusion controlled (Sangwal and Patel 1978, Bogenschultz et al, 1967). Usually the value of activation energy for a diffusion controlled mechanism is less than that of kinetically controlled one (Abramson and King 1939).

(a) Lactic acid :

High values of activation energy in case of lactic acid except for 0.7395N (5% by vol.) and 1.4790N (10% by vol.) concentrations above 40°C and for 10.353N (70% by vol.), 12.571N (85% by vol.) and 14.79N (100% by vol.) below 40°C, suggest that the mechanism of dissolution is kinetically controlled. The mechanism of dissolution near

the peak concentration i.e. 1.479N (10% by vol.) above 40°C is diffusion controlled. It is also diffusion controlled for higher concentrations (> 70% by vol.) below 40°C and is likely to be due to high viscosity of lactic acid (28.5 cp at 20°C). The details and causes for obtaining low values of activation energy near peak concentration (1.479N or 10% by vol.) are not yet well understood. An attempt is made to understand it by considering the nature of adsorption at the surface in section 5.4.3. It should be mentioned here that the values of activation energy for conductivity, E_c , and the values of activation energy for viscosity, E_η , are very low for almost all acids. It may be concluded here that for viscosity induced chemical process to be diffusion controlled due to viscosity only, following conditions should be satisfied :

$$\begin{aligned} E_t \text{ (or } E_s) &= E_c = E_\eta & \dots\dots (5.2) \\ n_t \text{ (or } n_s) &= n_c = n_\eta \end{aligned}$$

(b) Formic acid :

High values of activation energy for all concentrations of formic acid suggest that the mechanism of dissolution in case of formic acid is kinetically controlled one. Table 5.4 shows the viscosity of formic acid at various temperatures.

TABLE 5.4*

Temp. °C	Viscosity δ (cp)	$\log \delta$	$\frac{1}{T} \times 10^{-3}$
7.59	2.3868	0.3771	3.577
10	2.2620	0.3545	3.530
20	1.8040	0.2562	3.410
30	1.4650	0.1659	3.300
40	1.2190	0.0859	3.190
70	0.7800	1.8921	2.910
100	0.5490	1.7396	2.680

* Values taken from Handbook of Chemistry and Physics, CRC, Weast, 57th ed, 1976.

Fig. 5.14 shows the Arrhenius plot for viscosity of formic acid. The value of activation energy for viscosity, E_{δ} , is 0.16 ev. The value of activation energy for conductivity is 0.073 for 25.99 N (100% by vol.) formic acid. Thus the conditions for the process to be diffusion controlled, mentioned above, are not satisfied. Hence, the mechanism of dissolution in case of formic acid is kinetically controlled at all concentrations of formic acid.

5.4.3 Nature of adsorption :

Assuming the reaction to be catalytic one, the entire

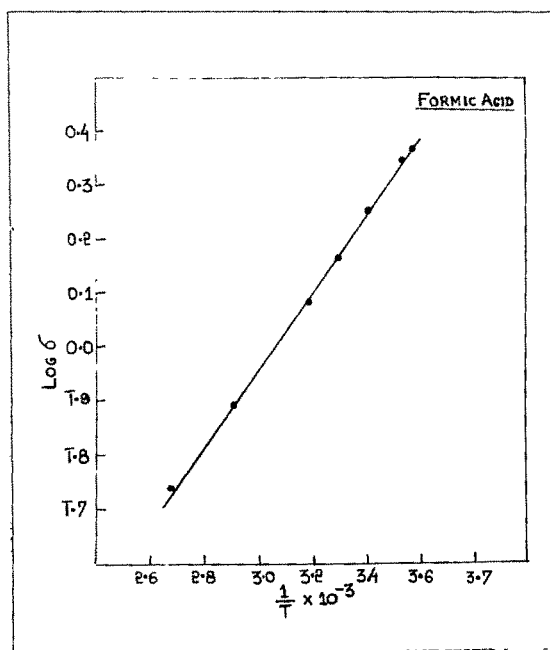


Fig. 5.14 Plot of $\log \sigma$ versus $1/T$ for formic acid.

process can be conveniently subdivided as follows :

(Gerasimov et al, 1974)

- (i) Adsorption of reactants on the surface,
- (ii) Transfer of adsorbed state into activated one
- (iii) Reaction in the adsorbed state with formation of products and
- (iv) Desorption of products.

Step (ii) requires the expenditure of energy, E_{true} , called true energy of activation of heterogeneous catalytic reaction. The apparent value of activation energy is given by,

$$E_{\text{cat}} = E_{\text{true}} - \Delta E \quad \dots \quad (5.3)$$

where ΔE is the enthalpy of adsorption. This equation suggests that when physical adsorption occurs, the value of E_{cat} is high and when chemisorption occurs, the value of E_{cat} is less. Thus, the drop in the value of activation energy near 1.479N (10% by vol.) lactic acid above 40°C may be due to the chemisorption of reacting and reacted species. It may be concluded here that the process of dissolution becomes diffusion controlled either due to chemisorption or due to very high viscosity of etchant as in case of lactic acid for concentrations greater than 10.353N (70% by vol.) below 40°C.

5.4.4 Concentration dependence of pre-exponential factors :

(a) Lactic acid :

Figs. 5.15 and 5.16 show the dependence of pre-exponential factors on concentration of lactic acid for tangential and surface dissolutions respectively. Pre-exponential factor varies with the concentration according to

$$A = A_0 C^m \quad \dots\dots (5.4)$$

The values of constant A_0 and slope m for different concentration regions below and above 40°C are computed from figs. 5.15 and 5.16. It should be mentioned here that the justification for drawing straight lines (figs. 5.15 and 5.16) is dependent on equation 5.4 and not on experimental values as there are very few points (observations) available on these plots. This remark is also applicable to observations made by employing different concentrations of formic acid. Further, no explanation is now available for splitting of the straight lines or for their intersecting point(s).

Using values of A_0 and m (figs. 5.15 and 5.16) Arrhenius equation for lactic acid can now be rewritten as follows :-

$$\begin{aligned} V_t &= 1 \times 10^{-3} C^{7.5} \exp(-E_t / KT) \\ V_s &= 1 \times 10^{-5} C^{3.3} \exp(-E_s / KT) \end{aligned} \quad \dots\dots(5.5)$$

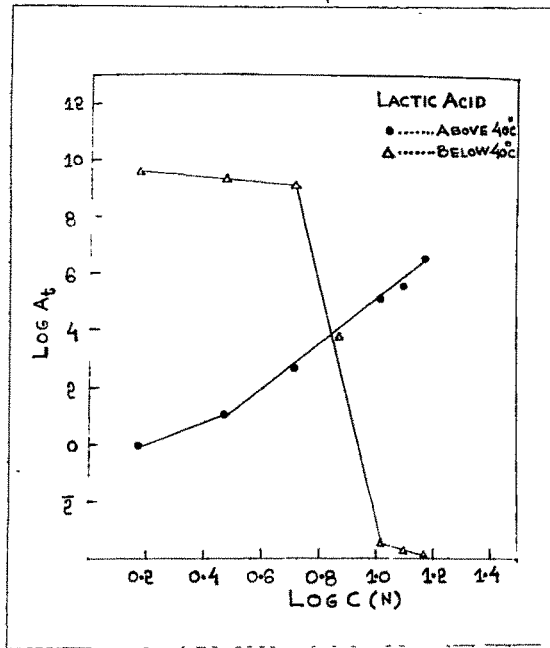


Fig. 5.15 Plot of $\log A_t$ versus $\log C$ for lactic acid.

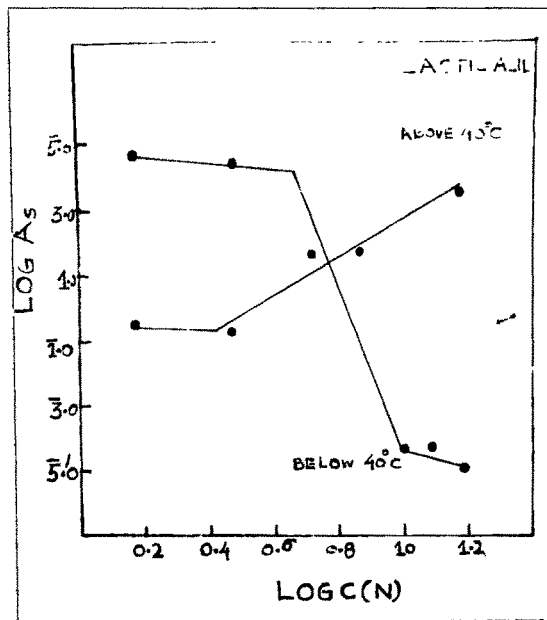


Fig. 5.16 Plot of $\log A_s$ versus $\log C$ for lactic acid.

for concentrations above 2.9580 N (20% by vol.) at temperatures greater than 40°C. For temperatures less than 40°C, the equations are

- (i) for concentration range 1.479N - 5.1765N (10% - 35% by vol.),

$$\begin{aligned} V_t &= 6.3 \times 10^9 C^{-0.9} \exp(-E_t / KT) \\ V_s &= 1 \times 10^5 C^{-0.2} \exp(-E_s / KT) \end{aligned} \quad \dots(5.6)$$

- (ii) for concentration range 5.1765N - 10.353N (35% - 70% by vol.),

$$\begin{aligned} V_t &= 10^{38} C^{-40} \exp(-E_t / KT) \\ V_s &= 10^{22} C^{-27.5} \exp(-E_s / KT) \end{aligned} \quad \dots\dots(5.7)$$

- (iii) for concentration range 10.353N - 14.79N (70% - 100% by vol.),

$$\begin{aligned} V_t &= 0.63 C^{-2.4} \exp(-E_t / KT) \\ V_s &= 10^{-2} C^{4.3} \exp(-E_s / KT) \end{aligned} \quad \dots\dots(5.8)$$

The rate of reaction is thus determined by activation energy as well as pre-exponential factors.

(b) Formic acid :

Plots showing dependence of pre-exponential factors A_t and A_s on concentration are shown in fig. 5.17. Similar equations for formic acid can be written as follows :

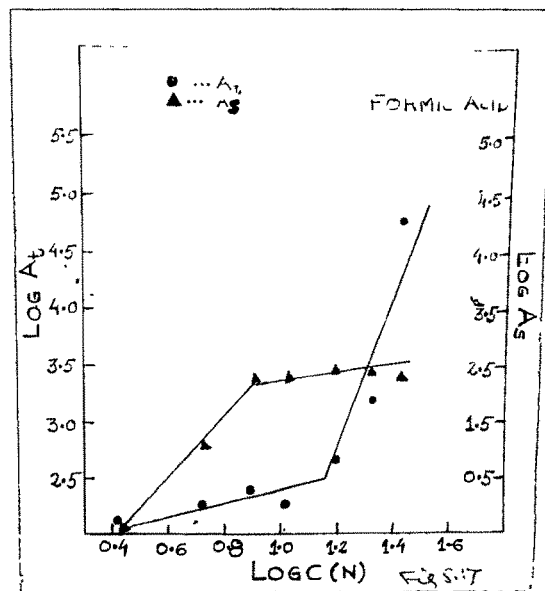


Fig. 5.17 Plot of log A versus log C for formic acid.

(i) for concentrations less than 15.494N (60% by vol.),

$$V_t = 56 C^{0.70} \exp(-E_t / KT) \dots (5.9)$$

$$V_s = 1 \times 10^{-3} C^{5.74} \exp(-E_s / KT)$$

(ii) for concentrations greater than 15.494N (60% by vol.),

$$V_t = 0.1 C^{3.5} \exp(-E_t / KT) \dots (5.10)$$

$$V_s = 2 \times 10^2 C^{0.13} \exp(-E_s / KT)$$

In general, the Arrhenius equation can be written as

$$V = A_0 C^m \exp(-E / KT) \dots (5.11)$$

Where A_0 is constant independent of concentration of the etchant. The concentration dependence of pre-exponential factors represented by equation 5.11 is in confirmity with the expression (Cabrera, 1956)

$$V = a \gamma_s \exp(-E_s / KT) \dots (5.12)$$

where V is the dissolution rate at an arbitrary point on the surface, a is the height of the step (10^{-8} cm), γ_s is the frequency factor characterizing the frequency of nucleation (which is supposed to depend on the number of molecules or ions of solvent striking the surface) and E_s is the activation energy of the formation of nucleus.

5.4.5 Temperature dependence of peak concentration :

It was mentioned earlier (section 4.3.4a, Chapter 4) that concentration at which maximum is obtained, C_{\max} , in V-C plots slightly depends upon the temperature in case of lactic acid. Table 5.5 shows the values of C_{\max} and corresponding temperatures of etching.

TABLE-5.5

Temp. °C	C_{\max} , N	$\frac{1}{T} \times 10^{-3}$	$\log C_{\max}$	$\log T$
20	0.7395	3.41	1.8689	2.4669
30	0.7395	3.30	1.8689	2.4814
40	1.4790	3.19	0.1700	2.4955
50	1.4790	3.09	0.1700	2.5092
60	1.4790	3.00	0.1700	2.5224
70	1.4790	2.91	0.1700	2.5353
80	2.9580	2.83	0.4700	2.5478

Fig. 5.18 shows the plot of \log of C_{\max} versus $1/T$. The graph is a straight line with slope 1038. Hence,

$$C_{\max} = K_1 \exp (- \text{slope} / T)$$

where K_1 is constant equal to 2.5×10^3 . Fig. 5.19 shows the plot of $\log C_{\max}$ versus logarithm of absolute

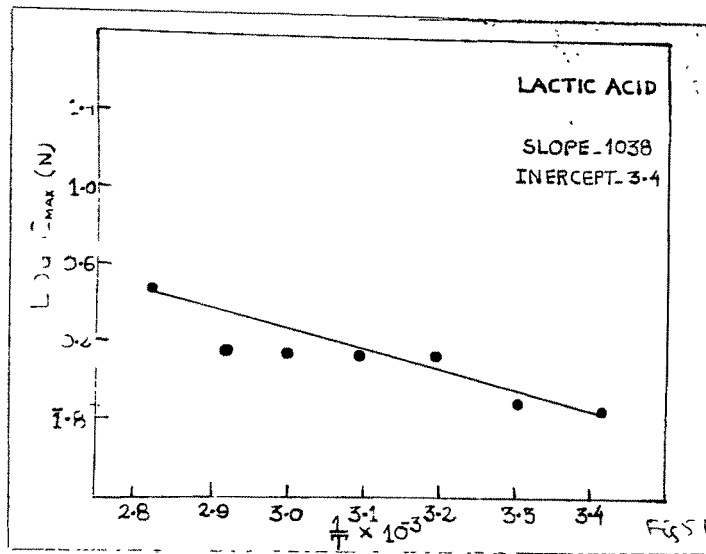


Fig. 5.18 Plot of $\log C_{max}$ versus $1/T$ for lactic acid.

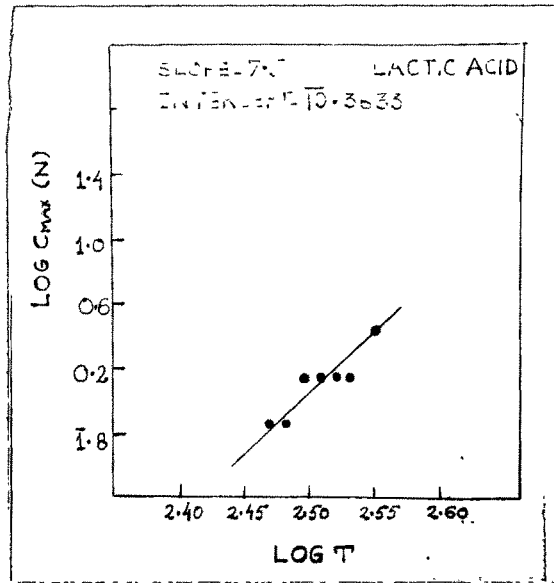


Fig. 5.19 Plot of $\log C_{max}$ versus $\log C$ for lactic acid.

temperature. The plot is again a straight line. Hence,

$$C_{\max} = K_2 T^a$$

where $K_2 = 2.308 \times 10^{-19}$ and $a = 7.50$. However, it could not be decided conclusively in what way C_{\max} varies with temperature because of inadequate number of observations and noticeable scattering of observations around approximated straight line plots (figs. 5.18 and 5.19). In case of formic acid, C_{\max} does not depend upon temperature.

5.5 CONCLUSIONS :

- (1) For a given concentration, shape of an etch pit depends on activation energy. However, the converse is not true.
- (2) For better quality of etch pits, the ratio E_t / E_s should have higher value.
- (4) Mechanism of dissolution becomes diffusion controlled either due to very high viscosity of the etchant or due to chemisorption.
- (4) For a process to be diffusion controlled, following conditions should be satisfied :

$$E_t \text{ (or } E_s) = E_c = E_\sigma$$

$$\text{and } \eta_t \text{ (or } n_s) = n_c = n_\sigma$$

(5) Arrhenius equation can be rewritten as

$$V = A_0 C^m \exp(-E / KT)$$

where A_0 is constant independent of the concentration of the etchant.